Kwan, J.S.H., Koo, R.C.H. & Ng, C.W.W. (2015) Landslide mobility analysis for design of multiple debris resisting barriers. Canadian Geotechnical Journal, Vol 52(9), pp 1345-1359

The Assessment Board selected this paper for the 2018 HKIE Geotechnical Paper Award, for its potential to advance local geotechnical practice and its quality of writing for the readership of practicing geotechnical engineers. It noted:

> The paper Kwan et al (2015) documents development of a methodology for rational design of multiple barriers for intercepting mobile landslide debris. It started with Newtonian mechanics, took hints from physical model tests and case records, demonstrated by application to a real design case, and benchmarked against an advanced numerical model. This comprehensive and solid approach won confidence. The proposed methodology promises to fill another gap in Hong Kong's continual search for more reliable and effective design of debris flow barriers. The paper is clearly and logically written, with the support of two very helpful appendices on aspects demanding greater details to make sense of the subject matter. It should be accessible to most geotechnical practitioners with a good grasp of basic mechanics.

General information of the article

Type of paper: Article

Title: Landslide Mobility Analysis for Design of Multiple Debris-resisting Barriers

Authors: J. S. H. Kwan, R. C. H. Koo* and C. W. W. Ng

*Corresponding author

Information of the authors

Co-author: Dr J. S. H. Kwan

Senior Engineer, Geotechnical Engineering Office, Civil Engineering and Development Department, Hong Kong SAR Government

E-mail: juliankwan@cedd.gov.hk

Corresponding author: Mr R. C. H. Koo

Engineer, Geotechnical Engineering Office, Civil Engineering and Development Department, Hong Kong SAR Government

E-mail: raymondchkoo@cedd.gov.hk

Co-author: Professor C. W. W. Ng

Chair Professor, Department of Civil and Environmental Engineering, Hong Kong University of Science and Technology, Clear Water Bay, Kowloon, Hong Kong.

E-mail: cecwwng@ust.hk

Abstract: Multiple debris-resisting barriers have been commonly used worldwide to mitigate debris flows in drainage lines. However, there lacks a well-developed methodology to assess the mobility of debris flows with consideration of the obstruction of the barriers. Free field debris flow condition which omits the presence of multiple debris-resisting barriers is commonly considered in design, although the effects of the barriers could be critical in determining the dynamics of landslide debris including debris velocity and debris thickness. This paper proposes a staged debris mobility analysis which accounts for the effects of multiple debris-resisting barriers. The staged analysis adopts solutions of depth-averaged debris mobility model. The input parameters of the analysis have been established from field data and laboratory test results. Rigorous numerical simulations of debris flows intercepted by multiple debris-resisting barriers have also been undertaken using three dimensional finite-element program LS-DYNA to provide results for benchmarking the output of the staged analysis.

Keywords: multiple debris-resisting barriers, landslide debris mobility analysis, debris flows, LS-DYNA.

Introduction

Multiple debris-resisting barriers (hereinafter referred to as multiple barriers) have been adopted in many countries to mitigate landslide hazards (WSL 2008; Shieh et al. 2006; Shum & Lam 2011). In general, multiple barriers comprise rows of single barrier installed at different strategic positions along the runout path of a given debris avalanche or debris flow. They are often built with a deposition area upstream to contain the debris. The barriers can be formed to different sizes and shapes to suit the topography, and a curved upstream surface may be provided to reduce the debris impact loading on the barrier (Shieh et al. 2006). Each row of single barrier is designed to retain a portion of landslide volume. Because of this, the scale of individual barriers, in terms of structural requirements and retaining height, could be optimized to cope with the site constraints and could also be more effective in minimizing entrainment (Wong 2009).

Experience suggested that multiple barriers can be a practicable means to mitigate reasonably large debris avalanches and debris flows. Various international publications give guidance and recommend good practice on certain design aspects of multiple barriers. For examples, CGS (2004) and NILIM (2007) provide guidelines for calculating retention volume of barriers, and SWCB (2005) recommends the minimum spacing between barriers. However, there are so far no well-established design guidelines for assessing the effect of the presence of multiple barriers on the landslide debris mobility.

Speerli et al. (2010) reported several debris flow flume tests to examine the dynamics of debris overflowing from small-scale ring-net barriers. A mixture of clayey gravelly sand and water was used in their tests. They observed that debris followed a ballistic projectile path after overtopping from the barrier and the debris was retarded upon impacting on the flume bed at the landing position. Debris would then accelerate when it propagated downstream along the inclined flume. Glassey (2013), who evaluated the effectiveness of the check dams

installed in the Illbach channel in Illgraben, Switzerland, mentioned that energy gain and energy dissipation are involved in the process of debris overflowing from filled-up barriers and debris landing. Glassey suggested that the height of check dams should be at least the height of debris flows.

Debris mobility assessment for design of multiple barriers calls for consideration of salient features involved in the debris runout process which include filling-up of barriers, overflowing from the barrier crest and energy dissipation at the debris landing position. This paper presents an analysis of debris mobility for the design of multiple barriers based on pertinent field and laboratory studies. To facilitate multiple barriers design, a staged mobility analysis is proposed to provide a means for assessing debris mobility dynamics taking into account the obstructions of multiple barriers. A debris mobility model developed using computer program LS-DYNA, calibrated against Yu Tung Road debris flow, has also been adopted to undertake debris flow simulations for benchmarking the results of the staged mobility analysis.

Dynamic analysis of landslide debris

In the design of multiple barriers, due to the lack of well-established methodology for assessing landslide debris dynamics, it has been assumed that the dynamics could be similar to that in the free-field conditions, i.e. presence of the multiple barriers is neglected. According to Wendeler et al. (2012), a series of 13 barriers was built along a drainage line to mitigate debris flow hazard in Switzerland, and the barrier design was established on the basis of the maximum debris velocity observed in the field. On the other hand, some researchers (e.g. Remaitre et al. 2008) have evaluated the influence of a series of filled-up barriers by considering variations in channel gradient. However, the analysis could not model reduction in debris volume and hence thickness due to debris retained by intermediate barriers.

In the prevailing geotechnical practice, dynamic mobility models have been used in the

design of debris-resisting barriers. With specific rheological parameters, numerical analyses can produce robust estimates of the dynamics of landslide debris for design purposes. Hungr et al. (2007) summarised details of various rheological and numerical models which were used in the debris mobility benchmarking exercise held in Hong Kong in 2007 and concluded that most of the common numerical models produced consistent results with the same specific rheological models.

Common numerical analyses for simulation of dynamics of landslide debris runout adopt continuum model developed based on depth-averaged shallow-flow equations. The formulations are made with reference to columns of debris mass above a sliding surface. DAN-W adopts this type of formulations to simulate the post-failure motion of rapid landslides. A pre-defined volume of soil or rock would change into a fluid and flows downslope, following a path of a defined direction and width. The model implements a one dimensional Lagrangian solution of the equations of motion and is capable of using several alternative rheological relationships (Hungr 1995). The model has been widely adopted in the engineering practice in Hong Kong for debris-resisting barrier design and landslide risk assessment purposes. Another numerical program DMM (stands for Debris Mobility Model), that allows input of channel section geometry in trapezoidal shape, was developed by Kwan & Sun (2006) based on modified formulations of Hungr (1995). This model has also been calibrated for used in Hong Kong. DAN-W is capable of simulating the ballistic flight of debris overshooting from vertical or sub-vertical runout paths, but DMM is not equipped with this function. Both DAN-W and DMM are Lagrangian models which discretise the landslide debris mass into inter-connected slices in their computations. The process of debris filling-up barriers and the subsequent overflow may not be realistically simulated due to the connectivity of the slices assumed in the formulations of the models.

Eulerian continuum models viz. FLO-2D (O'Brien et al. 1993; Bertolo & Wieczorek

2005) and Kanako-2D (Liu et al. 2012) have been used for assessing dynamics of debris flows. According to Liu et al. (2012), Kanako-2D is able to simulate changes in elevation of debris runout trail due to deposition or erosion. However, the simulation would not be applicable for situation when the flow velocity and flow depth change rapidly behind the barrier. In addition, simulation of ballistic flight of debris from the crest of the barrier is not included in the formulations of the model. Similar to Kanako-2D, the dynamics of debris ballistic flight is not explicitly simulated by FLO-2D. The discharge above barrier (or levee) is computed using weir flow equation.

The above commonly used computer programs adopt depth-averaged numerical scheme and the analyses are essentially two-dimensional. Three-dimensional continuum landslide mobility analyses have been undertaken by Crosta et al. (2007), who used an Eulerian-Lagrangian finite element code developed by Roddeman (2002). More recently, Yiu et al. (2012) reported the use of three-dimensional finite-element package LS-DYNA for landslide mobility assessment. LS-DYNA stands for Livermore Software – Dial-a-yield Nonlinear Analysis and it uses explicit time integration to study nonlinear dynamic problems. The package has been applied widely for stress and deformation analysis of structures subject to impacts. The program handles scalar advection in an Eulerian grid and solves equations of motion based on an Arbitrary Lagrangian-Eulerian (ALE) description of finite-element method. Landslide debris is assumed to be elasto-plastic which follows Drucker-Prager yield criteria. The computational domain was discretised into an array of hexahedral elements. The elements record the variables of acceleration, velocity, displacement, strain, stress and kinetic energy of landslide debris mass at various positions within the computational domain. Debris mass transport between elements follows the results of the ALE descriptions. The ground surface on which landslide debris travels on is modelled using rigid shell elements. Coulomb frictional rule was assumed at the interface between the landslide debris and the shell surface.

The LS-DYNA model was benchmarked against several well-documented laboratory and field studies, including the experiments of dry sand flows over irregular surfaces by Iverson et al. (2004) and the Yu Tung Road debris flow in Hong Kong (AECOM 2012). In the simulation of Yu Tung Road debris flow, an additional damping force proportional to the square of the debris velocity was applied in the LS-DYNA analysis to retard the debris motion. This damping force accounts for the energy loss due to the turbulence of debris flows. Its magnitude has been estimated with reference to the velocity-dependent resistance of the Voellmy rheology (ARUP 2013).

A staged analysis for assessment of landslide mobility

The commonly used computer programs which adopt depth-averaged scheme cannot simulate the entire process of debris filling up the retention zone of a barrier and subsequently overtopping the barrier. It is suggested that simulation of debris dynamics for the design of multiple barriers could be carried out based on a staged mobility analysis which adopts solutions of depth-averaged Lagrangian model. The stage analysis comprises the following key steps:

(i) carry out debris mobility analysis using a suitable program (e.g. DMM or DAN-W) to simulate the dynamics of landslide that travels from the source to the first barrier;

(ii) use the results of the mobility analysis to determine the velocity at which the debris will launch into a ballistic flight from the crest of the barrier;

(iii) calculate the geometry of the ballistic trajectory path and the debris velocity after landing;

(iv) carry out debris mobility analysis to model the landslide debris travelling from the landing position to the next barrier; and

(v) repeat Steps (ii) to (iv) until landslide debris reaches the terminal barrier.

When a landslide impacts on a barrier, a portion of the debris is trapped and retained

behind the barrier, which results in a kinetic energy loss of the debris flow. Once the barrier retention zone is fully filled, the remaining debris launches into a ballistic flight from the crest of the barrier, carrying the kinetic energy of the remaining landslide debris. For a robust estimate of the length of debris trajectory (x_i, see Fig. 1), the velocity at which the debris launches into a ballistic flight (see also Step (ii) above) may be taken as the maximum velocity of the remaining debris (v_m), assumed to be in horizontal direction. The v_m is taken as maximum velocity parallel to channel slope at location (x = 0, y = 0 in Figure B1) and assumed to act in horizontal direction.

In the most common situations, the above assumption would be conservative and produce a more critical x_i, since the surface of the debris deposit behind an intermediate barrier is likely to be sloping at a lower angle than the natural channel. Kwan (2012) had conducted a review of debris deposition angles behind barriers for the design of retention capacity from the field observations of many countries. The review showed that the range of deposition angles behind barriers is between 1/2 and 3/4 of natural channel bed. However, there may be rare cases where the angle of debris deposition behind a barrier would exceed the inclination of the natural channel due to reasons such as excavation into the channel to form a steeper profile for the purposes of increasing the retention volume (Kwan 2012).

The v_m value can be obtained from the velocity output of the debris mobility analysis. For example, if the Lagrangian type mobility model (e.g. DMM) is used, the mass blocks that would be trapped by the barrier would be those at the front of the debris chain with a volume equal to the retention capacity of the barrier, and the maximum velocity of the remaining mass blocks would be used for trajectory length calculation.

With debris launching velocity, v_m (in m/s) in horizontal direction, height of barrier, h (in m), and inclination of the ground profile, θ (in degree), the length of debris trajectory, x_i (in m) can be calculated using Eq. (1) below, which is derived from energy conservation principle

(see Appendix B):

$$(1) \quad x_i = \frac{v_{m2}}{g}\left[\tan\theta + \sqrt{\tan^2\theta + \frac{2gh}{v_{m2}}}\right]$$

The equation above provides a reasonable estimate as compared with the results of flume tests (see Appendix A). If v_m is acting at an angle rather than horizontal, the horizontal component of v_m can be input to Eq. (1) for calculation.

The debris velocity just before landing, v_r (in m/s), is calculated based on the kinetic energy of the remaining debris and the kinetic energy gained in the drop from height as follows (see Appendix B):

$$(2) \quad v_r = \sqrt{\frac{2\left[KE_r + m_r g\left(h + C_x x_i \tan\theta\right)\right]}{m_r}}$$

where m_r = mass of remaining debris (in kg), KE_r= kinetic energy of remaining debris (in J), and C_x = correction factor on x_i.

Under common circumstances, each of the intermediate barriers would be designed to retain a certain portion of the debris flow. The remaining debris mass (m_r) relates to the amount of debris that cannot be trapped by the barrier, i.e. the total volume of debris before hitting the barrier less the barrier retention capacity that can be taking into account the remaining debris from upstream slope that will overflow the barriers. m_r and kinetic energy of the remaining debris (KE_r) can be obtained based on the mass and velocity of the remaining mass blocks calculated from Lagrangian debris mobility analysis. If the barrier has been filled up completely by the debris materials previously, the retention capacity of the barrier should be ignored, and m_r and KE_r can be taken as the mass and the kinetic energy of the entire landslide debris. The dynamics of subsequent overflow can still be analysed using the proposed staged analysis, e.g. for calculations of the overflow trajectory and debris mobility

analysis between the debris landing location and the next barrier.

Essentially, the frontal portion of the debris flow travels at the highest velocity comparing with the portion behind. Experience shows that debris flow velocity attenuates from the frontal portion, and the rate of attenuation becomes smaller towards the rear end of the debris flow mass. It is therefore expected that the velocity within the remaining debris (i.e. within the m_r) would not varies significantly, and the use of m_r in establishing v_r can be considered reasonable. However, if short barrier height is used and the portion of debris retained is small, the use of frontal velocity of the remaining mass for establishing v_r would be more appropriate.

x_i is the maximum projectile distance which defines the landing position of the frontal portion of the remaining debris as it is calculated based on the maximum velocity of the remaining debris. Since the velocity of debris varies, a correction factor C_x is applied to x_i in the equation for the sake of calculating the average projectile length of the overflow. . Suggested values of C_x, correspond to the ratio of the rear velocity to frontal velocity of the remaining debris, are listed in Table 1. As field data for establishing C_x values are limited, the values presented in Table 1 are established based on a parametric numerical study of projectile lengths over different combinations of barrier height, debris velocity and inclination of run-out path (see Appendix B). The program 2d-DMM has been calibrated in a number of landslide debris flow cases in Hong Kong and overseas including the 2008 Yu Tung Road debris flow considered in the illustrative example presented in this paper (Kwan et al. 2013; Chan & Kwan 2012; Kwan et al. 2006). It is considered reasonable to use the well calibrated program 2d-DMM for parametric studies to derive C_x.

For carrying out the mobility analysis of landslide debris downstream as stated in Step (iv) above, an initial debris velocity is required. This velocity, v_i (m/s), can be obtained by resolving v_r as shown below (derivations of the equation refer to Appendix B):

$$v_i = Rv_r \cos\left[\left[\tan^{-1}\sqrt{\frac{m_r g\left(h + C_x x_i \tan\theta\right)}{KE_r}}\right] - \theta\right] \quad (3)$$

where R = velocity correction factor.

In order to consider the velocity reduction due to the debris impacting on the trail at the landing position, a correction factor of R should be applied to the above equation. The present study has analysed the results of the flume test by Choi & Ng (2013) with a view to determining a suitable value of R for design purposes.

The flume test was carried out using dry sand. Appendix A presents details of the test set-up. Instrumentation of the test included high speed cameras, laser sensors and photo sensors. High resolution images were captured during the test to investigate the dynamics of debris impacting and filling up the rigid barrier, then launching into a ballistic flight from the crest of the barrier and resuming its travel on the flume bed upon landing (see figures presented in Appendix A). The image data have been interpreted by the present study using the Particle Image Velocimetry (PIV) technique developed by White et al. (2003) for estimating the velocity reduction at landing.

Typical PIV results are presented in Fig. 2. It shows the velocity at the instant of about 0.5 second after the sand had impacted on the barrier. The sand overflowed from the crest of the barrier at a velocity of about 1 m/s and then launched into a ballistic flight. It followed a projectile trajectory and finally landed on the flume bed at a maximum distance of 0.21 m downstream of the barrier. Due to the release of the potential energy, the sand flow accelerated along the trajectory path. The maximum velocity was up to about 1.8 m/s immediately before landing. Upon landing, the sand flow travelled along the flume bed. The sand flow velocity was reduced after landing. The ratio of the velocity parallel to the flume bed after and before impact has been determined at various times during the test. This velocity ratio ranged from about 0.3 to 0.5. Appendix A presents detailed interpretation of the test

results.

It should be noted that dry sand is frictional and develops high flow resistance at the impact point, where the normal momentum of the falling mass creates a large normal force. In case of saturated materials in the field, however, such an impact may create high pore-water pressure in the debris, resulting in low effective normal stress and hence small flow resistance.

Flume tests involving ballistic trajectory of dry granular flow comprising rock blocks had been conducted by Yang et al. (2011). The rock blocks used in their experiments were of dimension of up to 0.1 m. According to Yang et al. (2012), the granular flows in their tests involved rolling and bouncing of large granular particles. These flume tests may replicate the dynamics of debris avalanche. They observed that the granular flow was subjected to velocity reduction upon landing on the flume bed. Yang et al. (2012) reported that the velocity immediately after and before landing ranged from 0.41 to 0.75 with an average of 0.65.

Head loss of wet debris flows dropping from height has been studied by Chen et al. (2009). They carried out measurements along debris transport channels equipped with drop structures, and suggested a formula for estimation of head loss of debris flow dropping from height. The velocity of the debris flows reported by Chen et al. (2012) ranged from 3 m/s to 6 m/s and the debris transport channels under their study were gently inclined (about 10°). Based on the suggested formula, it can be estimated that the ratio of velocity in the direction of the downstream channel after and before landing is in the order of 0.3 for debris flow of thickness ranging from 0.5 m to 1.5 m with a drop height of 2 m to 4 m.

In addition to the above, data reported by Glassey (2013) and videos of Illgarben debris flows available on internet at http://www.wsl.ch/fe/gebirgshydrologie/massenbewegungen/prozesse/murgang/videos/index_EN, http://www.youtube.com/watch?v=tjWZTP3u9d4, http://www.youtube.com/watch?v=OUtZVn2NwrY, and http://www.youtube.com/watch?v

=tjWZTP3u9d4 have been reviewed. Quantitative data has been determined for investigation on *R* factor. Overall, a range of *R* factor is between 0.3 and 0.75. The results are systematically presented in Table 2. The value of *R* correlates with channel base materials. It is noted that *R* factor for debris impacting on hard flume channel base varied between 0.5 and 0.7. However, when the flume channel filled up with the debris, the *R* factor could reduce to a range of 0.3 to 0.5. This phenomenon of *R* factor reduction is also observed in the field studies in China and Illgraben when the channel base is filled up with loose materials or debris. Comparisons between dry sand flows and wet debris flows show that the ranges of *R* factor are similar. It is expected that high water content would give a higher value of *R* factor because water would act as lubricant. However, the turbulence effects brought about by the water may contribute energy loss. The field cases in Illgraben with high water content of debris flows also give similar range of *R* factor between 0.4 and 0.7, except after the channel base is filled up with debris.All in all, the ratio of velocity parallel to debris trail after and before landing could range from 0.3 to 0.75. The flow dynamics of debris impacting on the ground is complex. More importantly, the actual water content, particle size distribution and characteristics of channel bed at landing location which affect the velocity reduction could vary significantly. It is not easy to define precisely a value of *R*. In view of the large uncertainties involved, a value of *R* on the high side, 0.7, is recommended.

Debris mobility analysis to model the dynamics of landslide debris travelling from the landing position to the next barrier would be carried out as per Step (iv) above. x_i, as mentioned above, gives the initial position at which the debris mobility analysis would commence, and v_i gives the initial velocity of debris for the subsequent analysis. Another two parameters, i.e. debris length (x_d) and debris thickness (h_m), are required for carrying out the analysis. The length of debris, x_d, is assumed to be the same as that of the remaining debris before the overflow (i.e. the length of mass blocks that would not be trapped by the barrier). If

the length of debris is greater than the length of debris trajectory (i.e. $x_d > x_i$), the debris is taken to extend backward from the point of landing to beyond the barrier for calculation purposes. Though this is an idealization, it is more robust for design as the debris would start motion again with a higher potential energy. An additional reason for adopting x_d as opposed to x_i is that the latter would have led to greater initial debris thickness for the subsequent mobility analysis which could result in unrealistic basal resistance particularly for a Voellmy rheological model (Hungr 1995).

Debris thickness, h_m, upon landing can then be determined based on the volume of the remaining debris and width of the runout trail. In order to simulate a greater debris frontal thickness as normally observed, it is suggested that the maximum thickness of the remaining debris at the debris front should be adopted. The thickness of the frontal one-fifth of the mass blocks is taken to be the maximum thickness of the remaining debris (i.e. if 50 mass blocks are used to model the whole landslide debris, 10 mass blocks at the frontal position is assigned to have the maximum thickness of the remaining debris). The debris thickness is then assumed tailing off at a profile which corresponds to a volume of the remaining debris.

With the four initial conditions viz. v_i, x_i, h_m and x_d as established above, separate landslide debris mobility analysis can start off from the landing position to the barrier downhill. The impact velocity of landslide debris at the downhill barrier can be then calculated.

Sensitivity analyses of barrier height and other parameters

Sensitivity analyses have been carried out for different combinations of barrier height from 1 m to 5 m and a range of launching flow velocities (v_m) from 4 to 10 m/s using the proposed staged analysis (see Equations 1 to 3) to investigate the effect to the debris velocity after landing (v_i). The slope inclination between 5^o and 30^o has been assumed. It is observed that multiple barrier system could be more effective in dissipating energy if short

barriers are used, as short barriers limit the energy gain of landslide debris during overflows. Another observation is that the ratio of v_i/v_m is not sensitivity in the ranges of parameters considered. Only 15% variation in v_i/v_m is observed.

Application of the staged mobility analysis

The application of the staged mobility analysis is demonstrated through an illustrative example pertaining to the design of debris-resisting barriers for protection of Yu Tung Road, Hong Kong from debris flow hazards. On 7 June 2008, a sizable channelised debris flow involving an active volume of about 3,400 m^3 occurred in a natural hillside catchment above Yu Tung Road. A video showing the debris flow event is available online at http://youtu.be/R2uTKyK1c9k. Different pulses are observed in the video that characterize the mobility of the debris flow. The proposed staged analysis can be applied to analyse the dynamics of the overflow and debris dynamics between the landing location and the next barrier. A detailed geotechnical investigation of the event is reported by AECOM (2012). The debris flow is referred to as Landslide No. 25 (LS08-241), Catchment No. 30 in AECOM's report.

Fig. 3 shows the catchment and the section of natural drainage line, taken after the debris flow event. The debris flow was a result of a massive landslide with a 2,350 m^3 failure volume at the head of the drainage line. Severe rainfall was one of the contributing factors of the landslide. The landslide materials entered into the incised drainage line (see also Fig. 3 and Fig. 4), mixed with surface runoff and developed into a debris flow with an additional volume of 1,000 m^3. The debris flow travelled about 600 m and disrupted the traffic of Yu Tung Road immediately downstream of the drainage line outlet.

Before the debris flow, landslide risk of the catchment had been identified and design of a rigid debris-resisting barrier was underway. Up-to-date, construction of the rigid barrier has completed. The barrier is located at the outlet of the drainage line (Chainage Ch 525 m; the

Chainage starts at the crown of the landslide scar). The design debris retention volume is taken as 3,500 m^3. In order to achieve this retention volume, a 7 m high barrier wall was built. Debris mobility analysis was carried out with an assumption that a volume of 3,500 m^3 ground mass would detach at the head of the drainage line to establish the debris impact velocity and debris thickness for design of the rigid barrier. A detailed back-analysis of the presented Voellmy parameters has been carried out by Kwan et al (2012) to best fit the observation of the Yu Tung Road case. Voellmy rheological parameters comprising basal friction coefficient of 0.14 (tan φ_b, where φ_b is 8°) and turbulence coefficient of 500 m/s^2 (Kwan et al. 2012) were adopted in the debris mobility analysis. The design debris impact velocity and debris impact thickness for the barrier at Ch 525 m are 8 m/s and 2.1 m respectively.

To demonstrate the applicability of the staged debris mobility analysis, it is assumed that two intermediate barriers at Ch 360 m and Ch 480 m were proposed and stage approach is used for calculation of the impact debris velocity and impact debris thickness of the two intermediate barriers. This serves as an example to illustrate how the proposed stages approach is used. The height of the intermediate barriers is 3 m. The corresponding retention volumes calculated following the guidelines stated in CGS (2004) are 780 m^3 and 700 m^3. With the two intermediate barriers, a smaller design debris retention capacity of the terminal barrier at Ch 525 m would be required, and the barrier wall height is estimated to be 4 m. The number of intermediate barriers and the barrier height adopted in this illustrative example have not been optimised. In real design exercise, the number and the height of barriers should be determined with consideration of the design retention volume, potential visual impact, cost effectiveness, site accessibility and the actual topography.

The staged mobility analysis was carried out using debris mobility program 2d-DMM (the latest version of 2d-DMM allows for debris mobility analysis with an initial debris velocity specified as required in the proposed staged analysis). The analysis started off with a

debris volume of 3,500 m^3 at the landslide source area (i.e. the head of drainage line) with a maximum thickness of about 3 m. Fig. 4 shows the runout profile adopted in the mobility analysis. The vertical scale of the landslide source thickness and barrier height has been exaggerated by 50 times for clarity. The same rheological parameters as those of the conforming design were used. The analysis ran until the debris reaches the first intermediate barrier at Ch 360 m. Using eqs. (1) to (3), the initial conditions for the next stage of landslide mobility analysis were established. The next stage analysis was then carried out commencing at the downstream of the barriers. The procedure repeated until landslide debris reaches the terminal barrier at Ch 525 m. With the stage analysis, the velocity and thickness of debris approaching each of the barriers were calculated. Key results and the initial conditions involved are summarised in Table 3.

The stage analysis aims to assess the dynamics of the landslide debris with consideration of the obstruction of multiple barriers. According to the results of the analysis, the design debris impact velocity and thickness for the terminal barrier are 7.3 m/s and 1.1 m respectively. Comparing with the design values established for no intermediate barriers, i.e. 8 m/s and 2.1 m, the analysis shows that the intermediate barriers could lead to a reduction of 9% in debris velocity and 52% in debris thickness.

However, construction of the first intermediate barrier could be a technical challenge because the barrier is required to resist relatively high impact velocity (12.0 m/s) and great impact thickness (2.8 m). This highlights the importance of location selection for building intermediate barriers. Ideally, intermediate barriers should be positioned at broad and flat portions of the drainage line, which provide favourable conditions for slowing down landslide debris.

In order to ensure the function of debris retention, routine maintenance e.g. regular debris clearance would be needed. If it is assessed to be appropriate, the multiple barriers

function as a series of check dams, clearance of landslide debris would not be required. The filled barriers would contribute to a less steep runout profile that helps to reduce mobility and runout distance of any subsequent landslide events.

Benchmarking with LS-DYNA analysis

A three dimensional debris mobility analysis using computer program LS-DYNA has been carried out. The analysis produces data for benchmarking the results of the staged mobility analysis. LS-DYNA model developed by Yiu et al. (2012) is adopted. The program handles scalar advection and solves equations of motion based on an Arbitrary Lagrangian-Eulerian (ALE) description of finite-element method. The runout distance of Yu Tung Road debris flow exceeds 600 m and the width of some sections of corresponding runout trail is over 30 m. The computational domain is discretised into an array of uniform hexahedral elements of dimensions 2 m (wide), 2 m (long) and 0.5 m (deep). Over 930,000 elements are used in the model.

Drucker-Prager yield criteria are assumed to describe the internal rheology of the debris flow. Key parameters which define the properties of the debris flow materials are listed in Table 4. ARUP (2013) reported that the analysis result is not sensitive to Poisson's ratio (υ). A typical value of υ of 0.3 is adopted.

The bulk density (ρ) and stiffness parameters, including E and υ, are found not sensitive to the results of the analysis (ARUP 2013). Typical values commonly adopted in geotechnical analysis for design purposes are therefore assumed (Kwan et al 2012). The Yu Tung Road debris flow was watery as shown in the video record and the sedimentology of the event could mainly comprise sandy and coarse materials (AECOM 2012). In theory, it is a cohesionless material. However, specification of a non-zero value of cohesion is required for LS-DYNA analysis. Therefore, a nominal value, or a very low value of cohesion, 0.1 kPa, is assumed. The internal friction angle (φ_{int}) affects the mobility of landslide debris in the LS-DYNA

analysis, and has been back-calculated based on the velocity determined from the video record and the super-elevation data mapped on site (see Fig. 5) based on the best-fit model parameters.

In addition to φ_{int}, resistance to landslide debris motions modeled in the analysis affects the simulated debris mobility. The resistance applied in the model comprises (i) basal friction at the interface of the landslide debris and the surface of the runout trail, and (ii) damping force proportional to the debris velocity. The basal friction is assumed to be of Coulomb type and is proportional to the normal stress acting at the debris/ground interface. Basal friction coefficient (tan φ_b, where φ_b is 8°) of 0.14 same as the 2d-DMM analysis is adopted. The damping force (F_d) is calculated as per eq. (4):

(4) $F_d = \xi_d \, m \, v^2$

where F_d is damping force, m is mass of debris, v is debris velocity, and ξ_d is proportional constant.

This damping force is applied to simulate the energy dissipation due to turbulence. In depth-averaged calculations, similar resistance, proportional to v^2, is considered in the Voellmy rheology (Hungr 1995). The turbulence resistance (F_{turb}) in the Voellmy rheology is defined as:

(5) $F_{turb} = m \, g \, v^2 / \xi \, h$

where F_{turb} is turbulence resistance, g is gravitational acceleration, h is debris thickness, and ξ is turbulence coefficient.

Voellmy rheology has proven to produce reasonable simulations of channelised debris flows (GEO 2011). The damping force applied in LS-DYNA analysis is therefore established with reference to the Voellmy rheology. The accelerations (or decelerations) resulted from F_d is pegged to that of F_{turb} (i.e. $F_d / m = F_{turb} / m$). It follows that

(6) $\xi_d = g / \xi h.$

According to GEO (2011), ξ should be taken as 500 m/s^2 for modeling channelised debris flows for design purposes. Using eq. (6) and on the basis of the field mapping results that the average debris thickness of the debris flow event is in the order of magnitude of 2 m, ξ_d for the LS-DYNA analysis is taken as 0.01 m^{-1}.

Fig. 5 shows the frontal debris flow velocity of Yu Tung Road debris flow calculated by 2d-DMM and LS-DYNA. Both numerical models produced comparable results which generally matched the debris velocity determined based on the video record and super-elevation data mapped in the field. The differences would be caused by the localised channel surface conditions which have not been modelled explicitly. Also, the water content of debris flow may also affect the turbulence effect on the velocity at certain locations with various topography conditions. It is difficult to obtain sufficient original specific information throughout debris flow path after the event had been occurred. In the light of information, a constant best-fit set of rheological parameters has been applied throughout the debris flow profile. Also, the field observations were estimated from the super-elevations instead of instrumental measurements which could be associated with some degrees of uncertainties. 2d-DMM and LS-DYNA adopt different numerical strategies. 2d-DMM is developed based on depth average approach, whereas LS-DYNA is a full 3-dimensional analysis with consideration of the yield criteria of the materials being modelled. The 2d-DMM analysis requires a pre-defined debris trail width whereas LS-DYNA does not. These factors may also contribute to the difference between the two simulation results. The internal friction angle (φ_{int}) used in the LS-DYNA analysis is 15°. The LS-DYNA analysis is undrained in nature, φ_{int} should be regarded as an apparent friction angle which incorporates the effects of pore water pressure. In view that the debris flow is watery, this back-calculated internal friction angle (i.e. 15°) is of a reasonable order of magnitude. In addition to debris

velocity, the LS-DYNA analysis reproduced debris flow length (~200 m) similar to that observed in the video and is consistent with the debris length (x_d) of the staged analysis (see Table 2 and Fig. 6). The maximum thickness of debris at Ch 360 m and Ch 480 m calculated by LS-DYNA analysis are 3.5 m and 2.5 m respectively. The calculated values are similar to the maximum debris thickness estimated in the field, which is between 2 m and 3m (AECOM 2012).

The calibrated LS-DYNA model has been modified to include two intermediate barriers at Ch 360 m and Ch 480 m. The barriers are modelled using rigid plate element, firmly attached to the topography. The barriers are 3 m high and assumed to be 2 m thick. Material properties and resistance parameters same as those adopted in the above calibration run are used. In contrast to staged analysis, LS-DYNA analysis simulates explicitly the dynamics of debris flows and debris retention behind intermediate barriers (see Fig. 7).

Fig. 8 shows the velocity vector plots of the flow field in the proximity of the first intermediate barrier at Ch 360 m. The figure reveals the debris flow dynamics involved and the debris-barrier interaction. When debris flow reaches the barrier, it is impeded by the obstruction of the barrier. Debris at the frontal portion runs up against the barrier. A plug is formed by the debris stopped and trapped behind the barrier. The extent of the plug develops when further debris is stopped behind the barrier. Debris flow subsequently rides on the plug and overtops the barrier. Debris overflowing from the barrier launches into a ballistic flight, and resumes its travel on the runout trail after landing.

Key results produced by the staged analysis and the LS-DYNA simulation are compared in Table 5. The adopted C_x value of the staged analysis is 0.8. The staged analysis generally gives results comparable with the LS-DYNA simulation, albeit on a relatively high side. The debris approaching velocity calculated by the staged analysis is 5% to 11% higher. Similarly, the thickness of debris approaching barriers calculated by the staged analysis is greater

compared with the LS-DYNA analysis. In addition, both LS-DYNA simulation and staged analysis give similar remaining kinetic energy of about 40% comparing to the free-field condition at the location of Ch 525 m, i.e. about 60% of kinetic energy is dissipated by the two multiple barriers. Usually, hydrodynamic equation would be used to calculate the dynamic impact pressure in sizing rigid barriers, of which the pressure is proportional to the velocity square. For this illustrative example, the difference in dynamic impact pressure obtained from the velocities of 2d-DMM and LS-DYNA is 20% maximum, which is considered acceptable in engineering design purpose.

Two sets of additional analyses assuming that intermediate barriers are 2 m and 4 m high respectively were carried out as a sensitivity study. It is observed that when smaller barriers of 2 m high are used, the debris impact thickness of the second and the terminal barrier is greater comparing with the 3 m high barriers, as the retention volume of the intermediate barrier is lesser. If higher intermediate barriers of 4 m high are used, the impact debris velocity and impact debris thickness of the second and the terminal barriers reduce by 15% and 10% respectively because of the reduction in the mass of overflow debris from intermediate barriers.

A sensitivity analysis has also been carried out using different combinations of internal friction angles of 5^o to 30^o. It is noted that when internal friction angle does not exceed 20^o, the effect of the internal friction angle on the calculated debris thickness is limited. However, when the internal friction angle is higher than 20^o, the calculated debris thickness increases with the internal friction angle. The reason may relate to the internal pressure of the debris mass. The internal pressure reduces with the internal friction angle, and the reduced internal pressure tends to result in a more intact debris mass i.e. less elongation and thicker debris mass.

Discussion

For the Yu Tung Road site, the staged analysis and LS-DYNA simulation produce comparable results for design of multiple barriers, although the results of the stage analysis is relatively higher on the debris impact velocity and thickness. The results of the staged analysis can be adjusted to match LS-DYNA's output by lowering the value of velocity correction factor R (see eq. (3)), as this will lead to a greater velocity reduction after landing. Nevertheless, calibration of the R value against LS-DYNA analysis for general use may not be appropriate because the R value would be dependent on the actual composition of the debris flow, and roughness and materials of the landslide trail at the debris landing location. The use of the recommended value of R (i.e. 0.7), which is on the high side of available data reported in literature, is selected with a view to achieving a suitably robust design of debris-resisting barriers.

The staged analysis has been undertaken using depth-averaged computer program. It is a simplified methodology for assessing dynamics of landslide debris that accounts for the obstruction of multiple barriers. Dynamic landslide simulations by advanced numerical package LS-DYNA provide a more complete picture of debris mobility against the barriers. It could provide insights pertinent to the understanding of landslide debris-barrier interaction and could stimulate advancement in engineering design of mitigation measures against debris flows. Continuous research and development work including validation and calibration of three-dimensional numerical models for assessing landslide debris dynamics could bring positive impacts to engineering practice.

Another two observations can be made based on the present study:

(a) Height of intermediate barriers should not be excessive - debris overflowing from a barrier launches into a ballistic flight. The overflowing debris gains potential energy and is not subject to any basal resistance during the flight at the same time. The gain would increase

when the debris runout path is steep, since a steeper runout profile would result in a larger drop height. In order to minimise the gain in potential energy, barrier height should not be too large. Otherwise, the impedance to debris flow brought about by the intermediate barriers may be off-set and a net increase in the kinetic energy of landslide debris may be resulted in. Glassey (2013) also mentioned that the distance of debris overflow should be limited because it would induce an increase in velocity. The present study is useful for practitioners to consider the flow dynamics and overflow mechanism for an effective barrier height design.

(b) Time delay in debris flow reaching outlet of drainage line - with presence of multiple barriers, landslide debris may take a longer time for travelling from the landslide source to the drainage outlet. The LS-DYNA simulation unveiled that Yu Tung Road debris flow might have reached the drainage outlet at 50 s after the onset of the landslide (see Fig. 6(f)). With the presence of intermediate barriers, 10 more seconds would be required for the landslide debris to travel from the landslide source to the drainage outlet (see Fig. 8(d); debris arrives at Ch 525 m at 60 s after landslide onsets). The additional time could be crucial in emergency situations because it could provide more lead time for the people/traffic affected to take emergency actions (e.g. road closure using automatic gate, etc.), albeit it appears to be limited. The time delay could be lengthened by placing additional intermediate barriers at suitable locations. With installation of a system of sensors to detect impacts of landslide debris on intermediate barriers for provision of early warning, the multiple barrier scheme could be a robust mitigation measure for managing landslide risk.

Conclusions

A staged debris mobility analysis which considers the obstruction of multiple debris-resisting barriers has been proposed. The staged analysis makes use of Lagrangian depth-averaged solutions computed by computer programs viz. DAN-W and 2d-DMM. The input parameters required for the staged analysis, e.g. correction factor to account for the

velocity reduction at landing, have been established on the basis of available experimental data reported in literature and results of flume test of dry sand flows.

In order to illustrate the applicability of the stage analysis, the design debris impact thickness and velocity of a multiple barrier scheme to mitigate debris flow site are calculated using the staged analysis. The results have been benchmarked with a three-dimensional dynamic landslide mobility assessment undertaken using LS-DYNA. The debris mobility model of LS-DYNA has been developed to consider turbulence resistance. Calibration of the LS-DYNA model is carried out using the debris velocity data corroborated by a video record and field mapping results. The results of the stage analysis and the LS-DYNA assessment are comparable, although the stage analysis produces higher design parameters in general.

The dynamics of debris flows obstructed by barriers are complicated, involving filling up and overflowing of barriers. The suggested staged mobility analysis is a simplified procedure which does not explicitly simulate these dynamics. The results generated are benchmarked with LS-DYNA analysis in one test site. Further review of the suitability of the staged analysis by means of field and laboratory experiments is worthwhile.

Acknowledgments

This paper is published with the permission of the Head of the Geotechnical Engineering Office and the Director of Civil Engineering and Development, Hong Kong SAR Government.

References

AECOM 2012. Detailed Study of the 7 June 2008 Landslides on the Hillside above Yu Tung Road, Tung Chung (GEO Report No. 271). Geotechnical Engineering Office, Hong Kong SAR Government.

ARUP 2013. Pilot Numerical Investigation of the Interactions between Landslide Debris and Flexible Debris-resisting Barriers. Report prepared for Geotechnical Engineering Office, Hong Kong SAR Government. ARUP (Hong Kong).

Bertolo, P. and Wieczorek, G.F. 2005. Calibration of numerical models for small debris flows in Yosemite Valley, California, USA. Natural Hazards and Earth System Sciences, **5**: 993-1001.

CGS 2004. Design Code for Debris Flow Disaster Mitigation Measures (DZ/T0239-2004)(Draft). China Geological Survey. (in Chinese)

Chan, Y.C. and Kwan, J.S.H. 2012. The state and practice of natural terrain landslide hazard mitigation in Hong Kong at 2012. *In* The Proceedings of the One Day Seminar On Natural Terrain Hazard Mitigation Measures, Hong Kong. *Edited by* CK Lau, Eddie Chan and Julian Kwan, pp 6-15.

Chen, X., Li, D. and Cui, P. 2009. Calculation buried depth of transverse sills for the debris flow drainage groove with soft foundation (in Chinese). Journal of Hefei University of Technology, **32**(10): 1590-1605.

Choi, C.E., and Ng, C.W.W. 2013. Flume Tests to Examine Dynamics of Debris Flows Obstructed by Baffles (Final Report). Report prepared for Geotechnical Engineering Office, Hong Kong SAR Government. The Hong Kong University of Science and Technology.

Crosta, G.B., Imposimato, S. and Roddeman, D. 2007. Approach to numerical modeling of long runout landslides. *In* Proceedings of the 2007 International Forum on Landslide Disaster Management (Volume II). *Edited by* Ken Ho and Victor Li. Geotechnical Division. The Hong Kong Institution of Engineers, pp 875-897.

Glassey, T. 2013. Hydrology and check dams analysis in the debris flow context of Illgraben torrent. MAS practical research project, Swiss Federal Institute of Technology Zurich, 103 p.

GEO 2011. Guidelines on the Assessment of Debris Mobility for Channelised Debris Flows (Technical Guidance Note No. 29). Geotechnical Engineering Office, Hong Kong SAR Government.

Hungr, O. 1995. A model for the runout analysis of rapid flow slides, debris flows and avalanches. Canadian Geotechnical Journal, **32**: 610-623.

Hungr, O., Morgenstern, N. and Wong, H.N. 2007. Review of benchmarking exercise on landslide debris runout and mobility modeling. *In* Proceedings of the 2007

International Forum on Landslide Disaster Management (Volume II). *Edited by* Ken Ho and Victor Li. Geotechnical Division. The Hong Kong Institution of Engineers, pp 755-812.

Iverson, R.M., Logan, M. and Denlinger, R.P. 2004. Granular avalanches across irregular three-dimensional terrain: 2. Experimental tests, Journal of Geophysical Research, **109**, F01015.

Kwan, J.S.H. (2012). Supplementary Technical Guidance on Design of Rigid Debris-resisting Barriers (Technical Note No. TN 2/2012). Geotechnical Engineering Office, Civil Engineering and Development Department, The HKSAR Government, 85 p.

Kwan, J.S.H., Chan, S.L., Chunk, J.C.Y. and Koo, R.C.H. 2013. A case study on an open hillside landslide impacting on a flexible rockfall barrier at Jordan Valley, Hong Kong. Landslides, DOI 10.1007/s10346-013-0461-x.

Kwan, J.S.H., Hui, T.H.H. and Ho, K.K.S. 2012. Modelling the motion of mobile debris flows in Hong Kong. *In* Landslide Science and Practice, Volume 3: Spatial Analysis and Modelling. *Edited by* C. Margottini, P. Canuti and K. Sassa. Springer-Verlag Berlin Heidelberg, pp 29-35.

Kwan, J.S.H. and Sun, H.W. 2006. An improved landslide mobility model. Canadian Geotechnical Journal, **43**: 531-539.

Liu, J., Nakatani, K. and Mizuyama, T. 2012. Effect assessment of debris flow mitigation works based on numerical simulation by using Kanako 2D. Landslides, **10**(2): 161-173.

NILIM 2007. Manual of Technical Standard for Establishing Sabo Master Plan for Debris Flow and Driftwood (Technical Note of NILIM No. 364). Natural Institute for Land and Infrastructure Management, Ministry of Land, Infrastructure and Transport, Japan. (in Japanese)

O'Brien, J.S., Julien, P.Y. and Fullerton, W.T. 1993. Two-dimensional water flood and mudflow simulation. Journal of Hydraulic Engineering, **119**(2): 244-261.

Remaitre, A., Van Asch, Th. W.J., Malet, J.P. and Maquaire, O. 2008. Influence of check dams on debris-flow run-out intensity. Natual Hazards and Earth System Sceinces, **8**: 1403-1416.

Roddeman, D.G. 2002. TOCHNOG User's Manual – A Free Explicit/implicit FE Program. FEAT. (www.feat.nl/manuals/user/user.html)

Shieh, C.L., Ting, C.H. & Pan, H.W. 2006. The impulsive force of debris flow on a curved dam. Proceedings of the Interpraevent International Symposium on Disaster Mitigation of Debris Flows, Slope Failures and Landslides, Niigata, Japan, pp 177-186.

Shum, L.K.W. & Lam, A.Y.T. 2011. Review of Natural Terrain Landslide Risk Management

Practice and Mitigation Measures, Technical Note TN 3/2011, Geotechnical Engineering Office, The Civil Engineering and Development Department, The HKSAR Government, 168 p.

Speerli, J., Hersperger, R., Wendeler, C. and Roth, A. 2010. Physical modeling of debris flows over flexible ring net barriers. *In* Proceedings of the Seventh International Conference on Physical Modelling in Geotechnics (ICPMG), Zurich, Switzerland. *Edited by* Sarah Springman, Jan Laue and Linda Seward. Taylor & Francis Group, pp 1285-1290.

SWCB 2005. Soil and Water Conservation Handbook. Soil and Water Conservation Bureau of the Council of Agriculture, Executive Yuan and Chinese Soil and Water Conservation Society. (in Chinese)

Wendeler, C., Haller, B. and Salzmann, H. 2012. Protection against debris flows with 13 flexible barriers in the Milibach River (Canton Berne, Switzerland) and first event analysis. *In* Proceedings of AGS Seminar on Natural Terrain Hazards Mitigation Measures, 16 October 2012, Hong Kong. *Edited by* C.K. Lau, Eddie Chan and Julian Kwan. The Association of Geotechnical and Geoenvironmental Specialists (Hong Kong), pp 22-28.

White, D.J., Take, W.A. and Bolton, M.D. 2003. Soil deformation measurement using particle image velocimetry (PIV) and photogrammetry. Geotechnique, **53**: 619-631.

Wong, H.N. 2009. Rising to the challenges of natural terrain landslides. *In* Proceedings of the HKIE Geotechnical Division Annual Seminar 2009. Geotechnical Division. The Hong Kong Institution of Engineers, pp 15-53.

WSL 2008. Integral Risk Management of Extremely Rapid Mass Movements. Swiss Federal Institute for Snow and Avalanche Research (http://irasmos.slf.ch/).

Yang, Q., Cai, F., Ugai, K., Su, Z., Huang, R. and Xu, Q. 2012. A simple lumped mass model to describe velocity of granular flows in a large flume. Journal of Mountain Science, **9**: 221-231.

Yang, Q., Cai, F., Ugai, K., Yamada, M., Su, Z., Ahmed, A., Huang, R. and Xu, Q. 2011. Some factors affecting mass front velocity of rapid dry granular flows in a large flume. Engineering Geology, **122:** 249-260.

Yiu, J., Pappin, J., Stuart, R., Kwan, J.S.H. and Ho, K.K.S. 2012. Landslide mobility and flexible barrier modeling using LS-DYNA. *In* Proceedings of AGS Seminar on Natural Terrain Hazards Mitigation Measures, 16 October 2012, Hong Kong. *Edited by* C.K. Lau, Eddie Chan and Julian Kwan. The Association of Geotechnical and Geoenvironmental Specialists (Hong Kong), pp 67-77.

Tables

Table 1. Suggested Values of C_x

Ratio of rear velocity to frontal velocity of the remaining debris	C_x
< 0.2	0.6
0.2 to 0.66	0.8
≥ 0.67	1.0

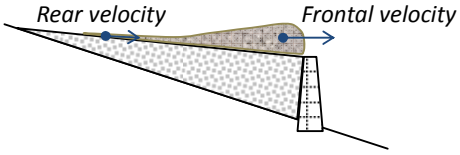

Table 2. R factor determined from the field and laboratory tests

Cases	Water content	Bedding	Water in channel at impact	Channel gradient	R factor
1. Bouldery granular flow* (Yang et al, 2011)	Dry	Hard flume base	No	10°	0.4-0.7
2. Debris flow mixture from clay to gravel* (Speerli et al, 2010)	25-30% by mass	Hard flume base	No	9° - 14°	0.5-0.7
3. Sand flow* (Choi & Ng, 2013)	Dry	Hard flume base (1st surge)	No	26°	0.5
		Sand base			0.3-0.4
4. Watery debris flow# (Chen et al, 2009)	High	Soft channel base	Yes	10°	0.3
5. Bouldery granular flow# (Information from the Illgraben debris flows observations in Switzerland on 3 June 2000, 28 June 2000, 22 July 2013 and 28 July 2014)	50% by volume	Gravelly base (1st surge)	Yes	5°-10°	0.4-0.7
		Bouldery deposit (rear surges)			0.3-0.5

Notes:

*Experimental flume tests

#Field tests

Table 3. Key results and initial conditions involved in the staged mobility analysis

		First intermediate barrier (Ch 360 m)	Second intermediate barrier (Ch 480 m)	Terminal barrier (Ch 525 m)
Design parameters	**Debris approaching velocity**	12.0 m/s	8.3 m/s	7.3 m/s
	Debris approaching thickness	2.8 m	1.9 m	1.1 m
Initial conditions for next stage analysis starts at downstream of the barrier	v_i	10.4 m/s	6.1 m/s	---
	x_i	15 m	7 m	---
	h_m	3 m	3 m	---
	x_d	192 m	186 m	---

Table 4. Key parameters of material property

Material property	**Parameter**
Bulk density, ρ	1,900 kg/m^3
Elastic modulus, E	10 MPa
Poisson's ratio, υ	0.3
Internal friction angle, φ_{int}	15°
Apparent cohesion, c	1 kPa

Table 5. Comparison between the results of the staged analysis and the LS-DYNA analysis

	Ch 360 m		Ch 480 m		Terminal Barrier	
	Debris approaching velocity	**Debris approaching thickness**	**Debris approaching velocity**	**Debris approaching thickness**	**Debris approaching velocity**	**Debris approaching thickness**
Staged Analysis	12.0 m/s	2.8 m	8.3 m/s	1.9 m	7.5 m/s	1.1 m
LS-DYNA	11.0 m/s	1.5 m	7.9 m/s	1.1 m	6.7 m/s	1.0 m

List of figures

Fig. 1. Design parameters for assessing dynamic motion of landslide debris overflowing from barrier

Fig. 2. Debris overflows from crest of rigid barrier

Fig. 3. Catchment of the Yu Tung Road debris flow

Fig. 4. Runout profile of the mobility analysis

Fig. 5. Frontal debris flow velocity against chainage using the best-fit model parameters

Fig. 6. Simulation of Yu Tung Road debris flow using LS-DYNA analysis

Fig. 7. Simulation of debris flow obstructed by multiple barriers

Fig. 8. Simulation of debris flow velocity vector plots (barrier at Ch 360 m)

Figures

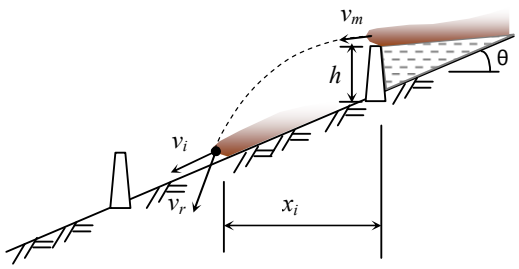

x_i = horizontal length of debris trajectory

v_m = debris launch velocity

v_r = debris velocity just before landing

v_i = debris velocity after landing, parallel to runout path

θ = inclination of runout path

h = height of barrier

Fig. 1. Design parameters for assessing dynamic motion of landslide debris overflowing from barrier

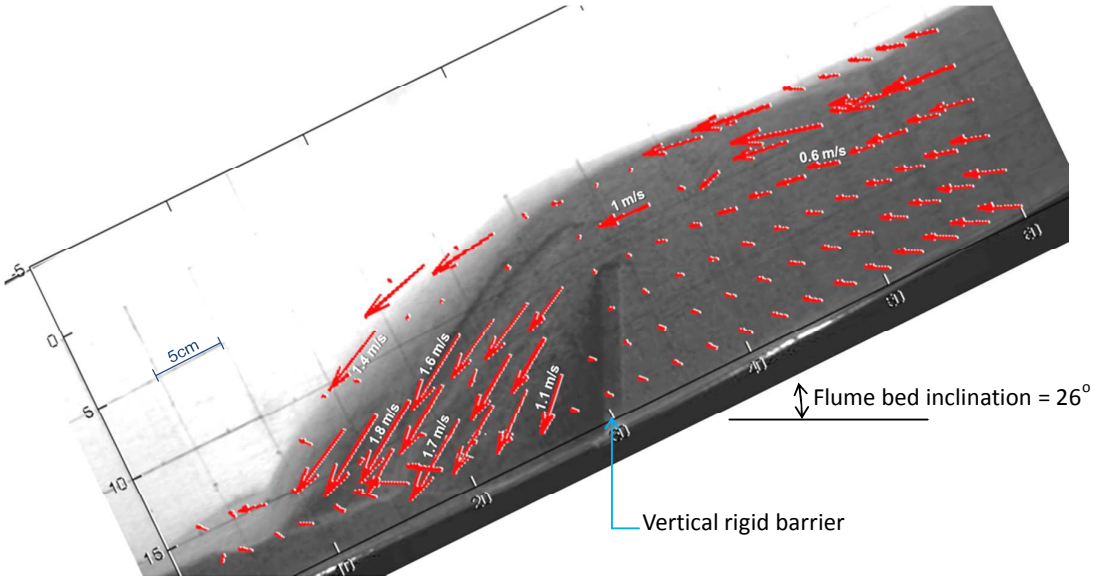

Fig. 2. Debris overflows from crest of rigid barrier

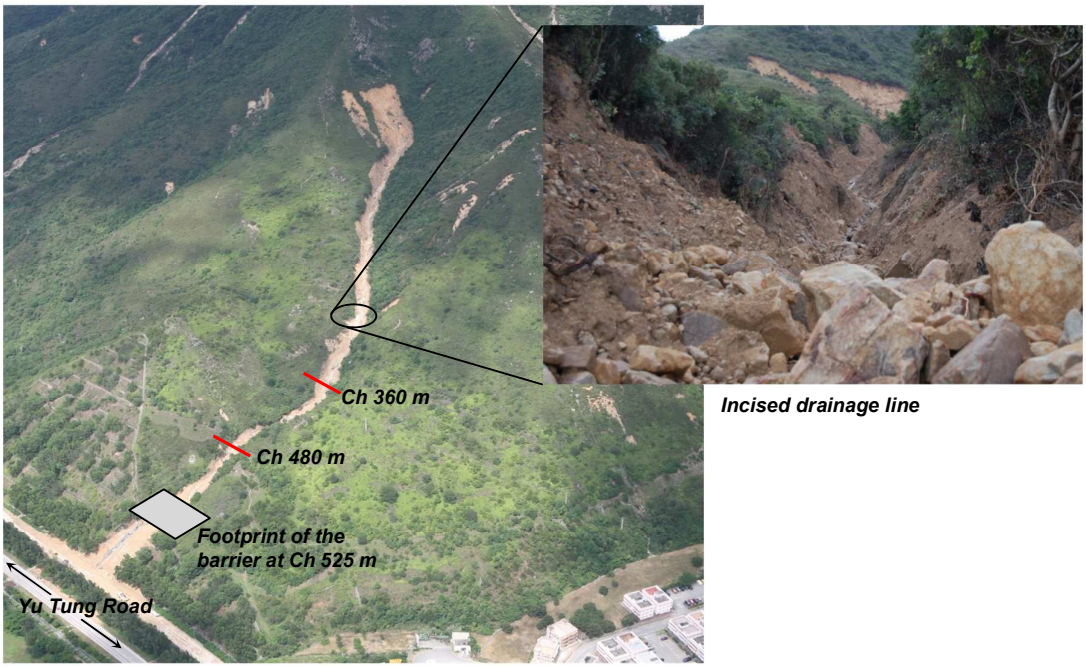

Fig. 3. Catchment of the Yu Tung Road debris flow

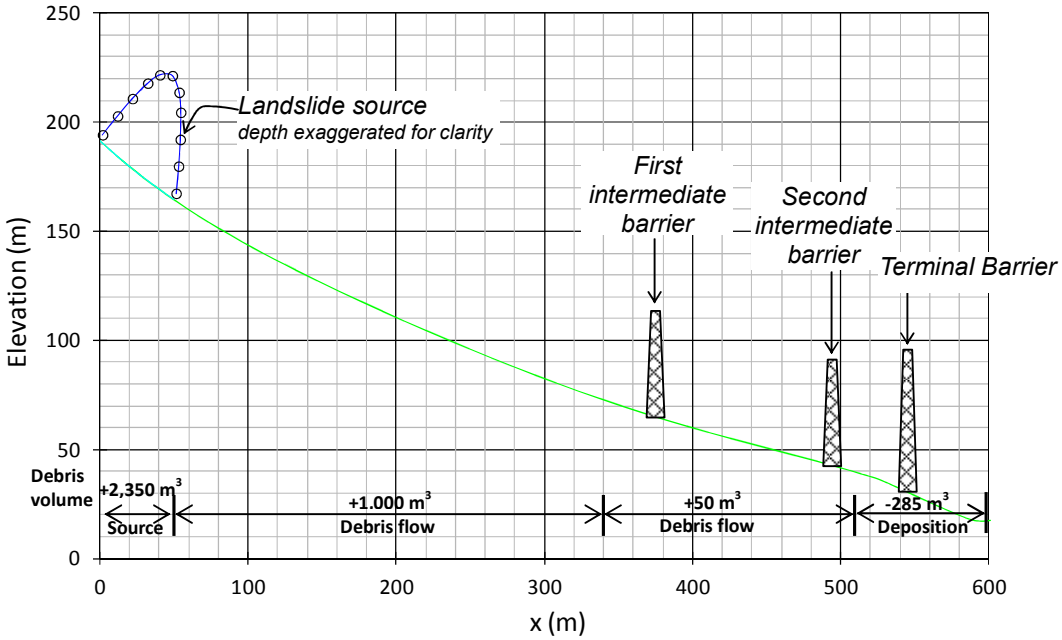

Fig. 4. Runout profile of the mobility analysis

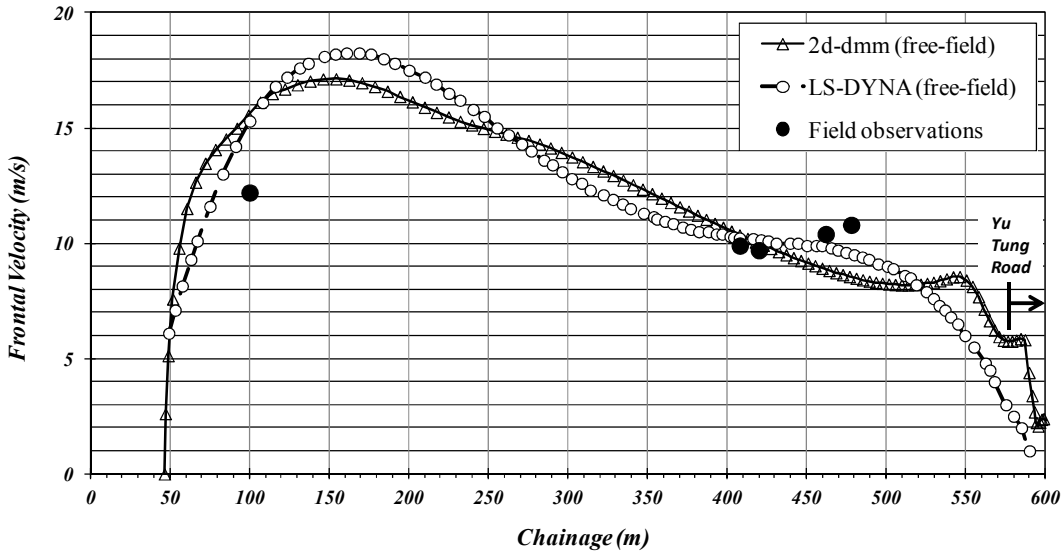

Fig. 5. Frontal debris flow velocity against chainage

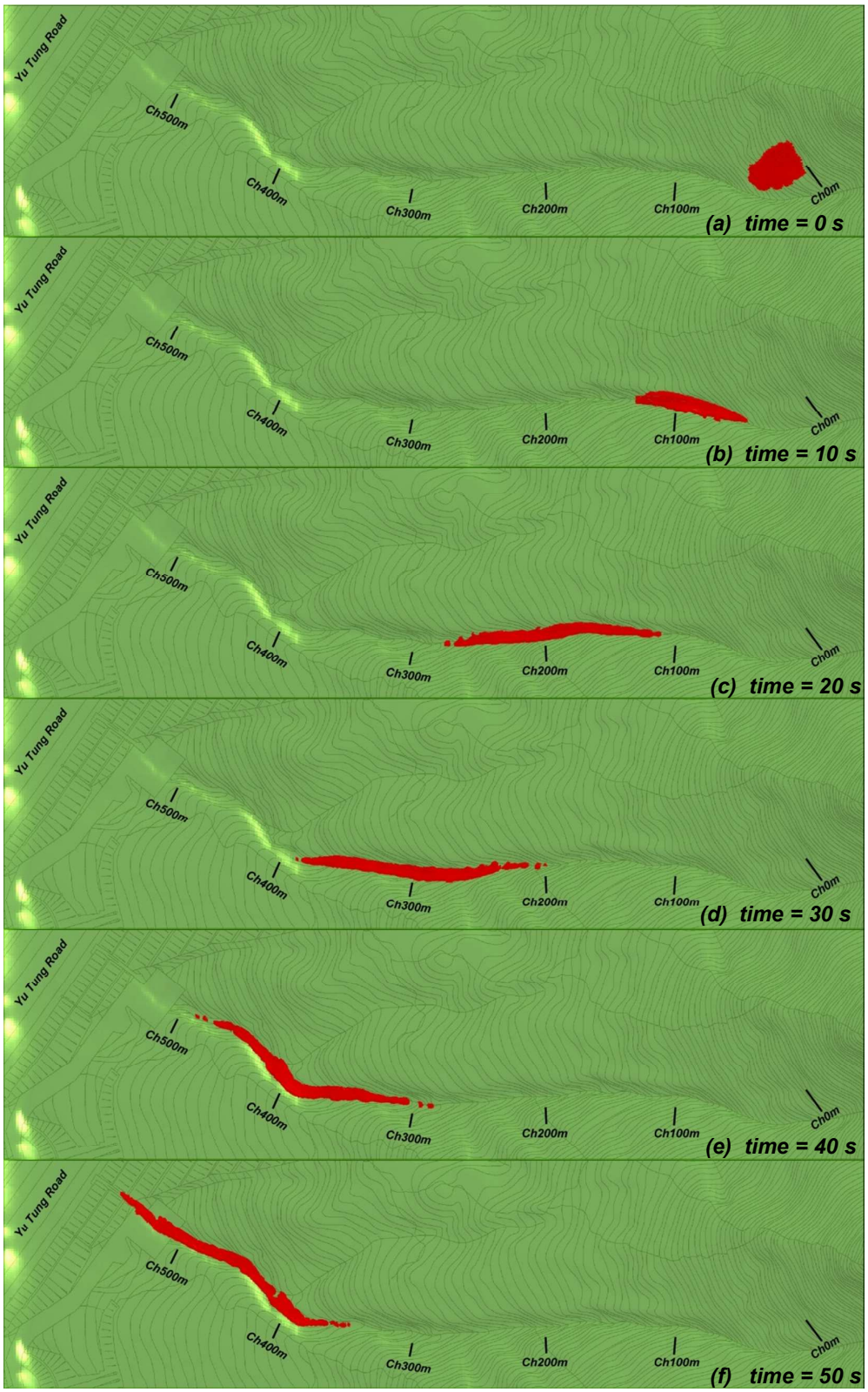

Fig. 6. Simulation of Yu Tung Road debris flow using LS-DYNA analysis

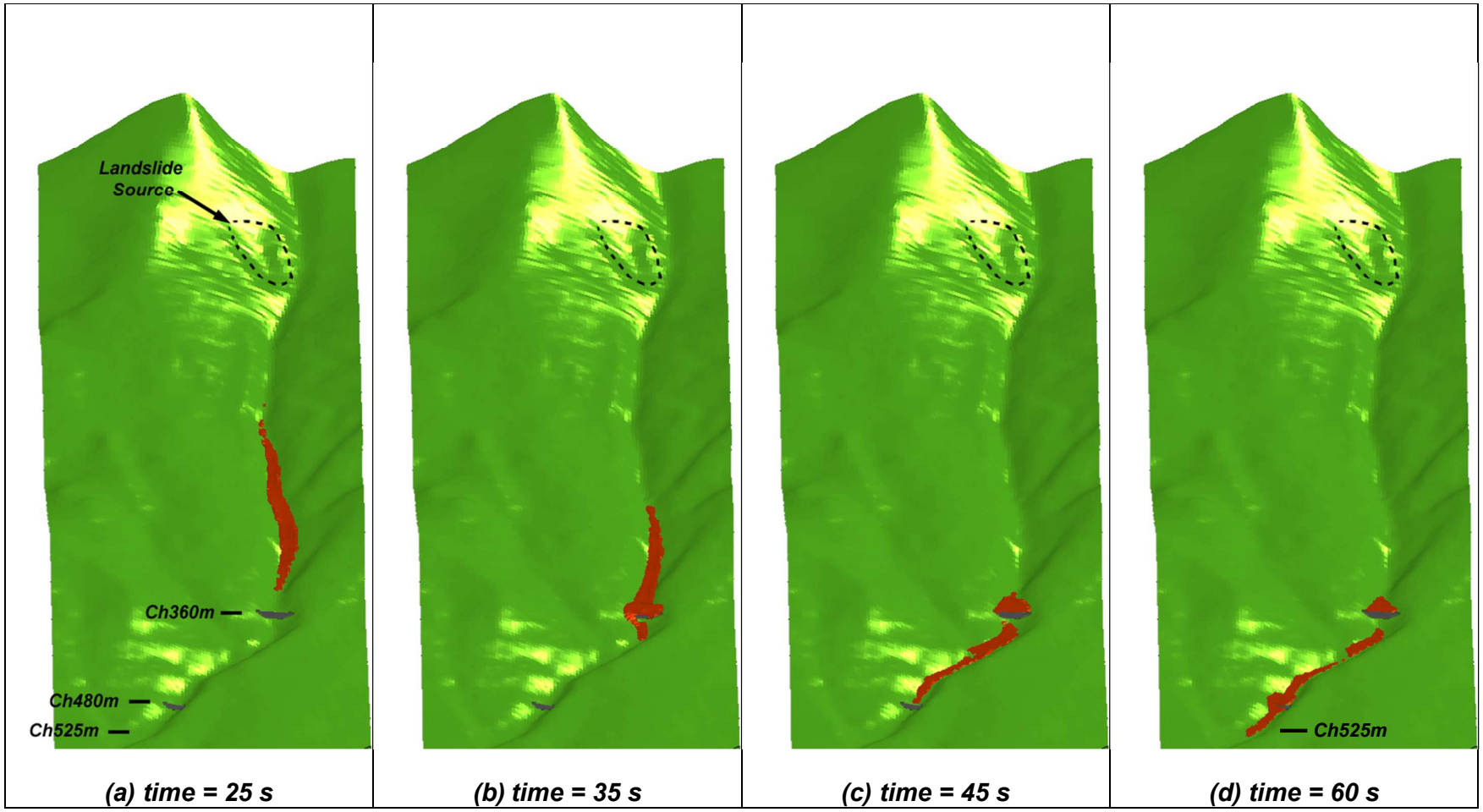

Fig. 7. Simulation of debris flow obstructed by multiple barriers

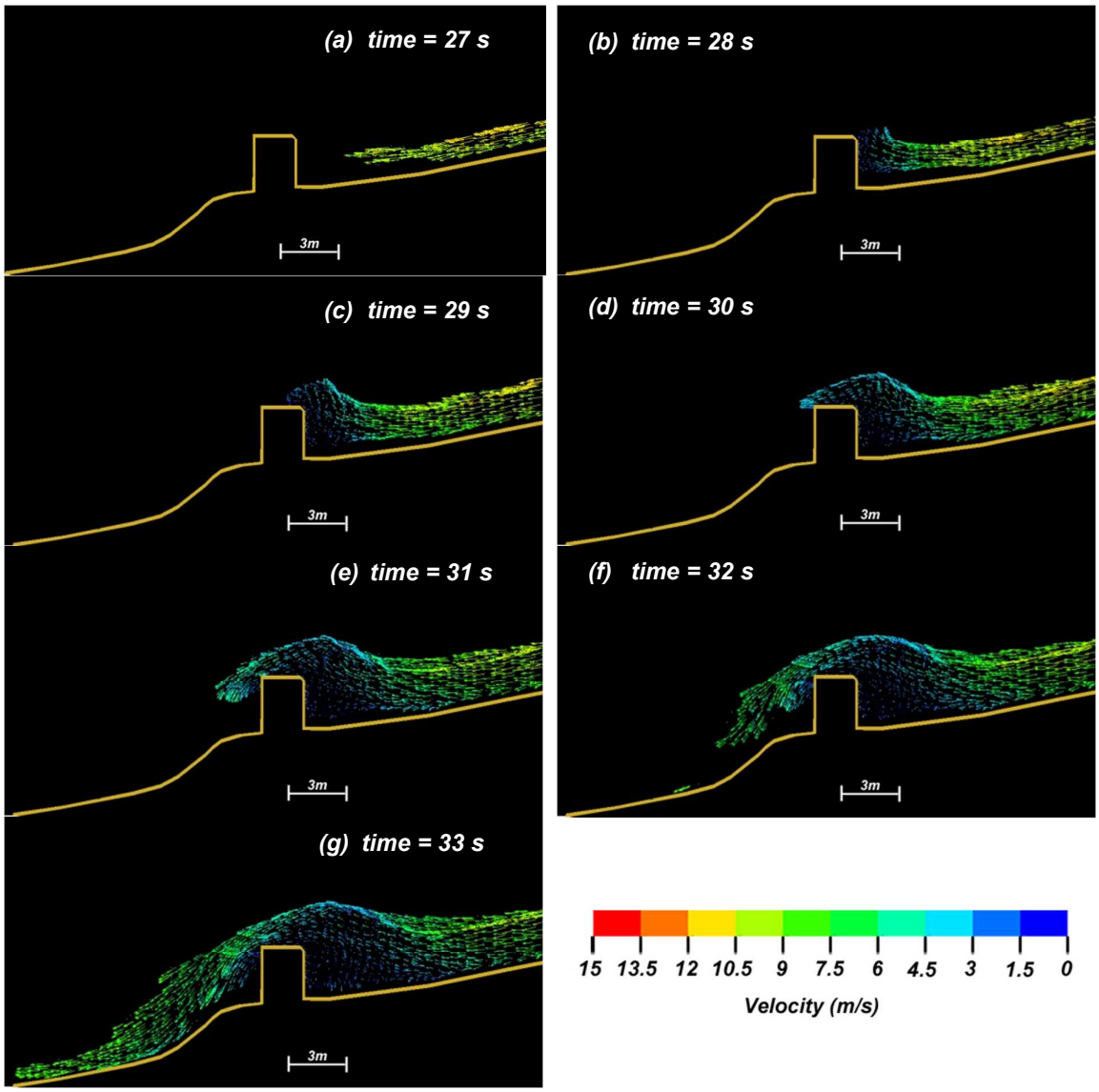

Fig. 8. Simulation of debris flow velocity vector plots (barrier at Ch 360 m)

Appendix A

A Flume Test of Landslide Debris Overflowing from Rigid Barrier

Introduction

The test was carried out in a 5 m long flume with a channel base width of 0.2 m. Side walls are about 0.5 m in height, perpendicular to the channel bed. Dry Leighton Buzzard Fraction C sand is composed of fairly uniform silica grains with specific gravity of 2.65 g/cm^3, was used in this series of flume tests. The particle size of the sand ranges between 300 μm and 600 μm. The angle of repose of the sand is 33° and the friction angle between the sand and flume bed is 23°. The initial bulk density of the sand mass is about 1680 kg/m^3. At the top end of the flume is a sand storage tank. Sand can be released into the flume by opening a flip gate that is attached to the tank. Details of the flume and the sand release mechanism are presented in Choi et al. (2014).

The vertical barrier model used in the flume test is 0.1 m high and made up of a 10 mm thick aluminum plate. It is firmly secured within the flume at midway of the channel. The scaling factor of the wall dimension is about 1/50 to typical prototype.

Several trials were carried out to establish an appropriate flume inclination. It was subsequently decided that the flume should be inclined at 26° based on the consideration of the Froude number of the sand flow. Froude number ($F_r = v / (g\ h)^{0.5}$, where v is debris velocity, g is gravitational acceleration and h is debris depth normal to the flume bed) is a dimensionless parameter usually adopted to characterise the inertia of debris flow. In design practice of Hong Kong, the value of F_r of debris flows in typical design scenarios for barrier design is about 3, given that design impact velocity is about 10 m/s and a flow depth of about

1 m (i.e. F_r = 10/ (10 x 1)$^{0.5}$ = 3.2). When the inclination of the flume is 26°, the sand flow in the flume would attain a velocity of about 2.6 m/s with an approaching depth of around 0.08 m at the location of the model barrier. This corresponds to a Froude number of 2.9 (= 2.6 / (10 x 0.08)$^{0.5}$). A series of experiments with different source volumes of dry sands overflow the rigid barrier has been carried out. The range of R factors observed from the experiments has been reported.

Experimental Results

The flume test was recorded with the use of a high-speed camera which could capture 100 images per second. Figure A1 shows the image records in sequence.

Fig. A1(a) shows the instant when the dry sand flow arrived at the barrier location. For discussion purposes, the time of this instant is denoted as t = 0.0 s. After 0.1 second, the sand flow filled up the retention zone behind the barrier and splashing of the sand is also evident. At t = 0.25 s, debris that was not trapped behind the barrier started the overtopping process and launched into a ballistic flight. Subsequently, debris overflowing from the crest of the barrier travelled along a projectile path and landed on the flume bed at a distance about 0.2 m downstream of the barrier (see Fig. A1(d)). This process continued for about 16 seconds. At the end of the test, sands piled up behind the barrier and the deposition angle was about 33°.

In this present study, the velocity of the sand flow has been determined using the 'geoPIV' computer package developed by White et al. (2003). This package is developed based on close-range photogrammetry techniques capable of tracking movements of soil grains captured in high-resolution images. It produces displacement and velocity vectors of the soil grains. Typical results of the PIV analysis are shown in Fig. 2.

Velocity Reduction at Landing

Velocity reduction upon immediate landing at the end of the ballistic flight has been

studied. Table A1 summarises the velocity parallel to the flume before and after landing as well as the velocity ratio. The velocity ratio ranges from about 0.3 to 0.5.

Projectile Length

Eq. 1 is developed to calculate the length of projectile for debris overflowing from the crest of barrier. The velocity and trajectory length data presented in Fig. 1 are used to verify this equation. As shown in the figure, debris overflowing velocity at the barrier crest is about 1.0 m/s. Using Equation 1, the estimated length of trajectory is 0.18 m. The trajectory length as observed in the test was 0.2 m. The difference of the trajectory length between the calculated value by eq. 1 and laboratory observation is within 10%, which is considered to be acceptable. However, the predicted result on reality may have larger discrepancy, since the debris materials and scale of barriers could be quite different to the laboratory test.

References

Choi, C.E. and Ng, C.W.W. 2013. Flume Tests to Examine Dynamics of Debris Flows Obstructed by Baffles (Final Report). Report prepared for Geotechnical Engineering Office, Hong Kong SAR Government. The Hong Kong University of Science and Technology.

Choi, C.E., Ng, C.W.W., Song, D.G., Kwan, J.S.H., Shiu, H.Y.K., Ho, K.K.S. and Koo, R.C.H. 2014. Flume investigation of landslide debris resisting baffles [online]. Canadian Geotechnical Journal, doi: 10.1139/cgj-2013-0115.

White, D.J., Take, W.A. and Bolton, M.D. 2003. Soil deformation measurement using particle image velocimetry (PIV) and photogrammetry. Geotechnique, **53**: 619-631.

Table

Table A1. Velocity data for calculating velocity reduction at landing

Time (s)	Velocity Parallel to the Flume Just Before Landing (V_b) (m/s)	Velocity Parallel to the Flume Immediately After Landing (V_a) (m/s)	V_a / V_b
0.46	1.3	0.6	0.46
0.51	1.4	0.6	0.43
0.61	1.6	0.7	0.44
1.11	1.6	0.4	0.25
1.31	1.3	0.4	0.31

Figure

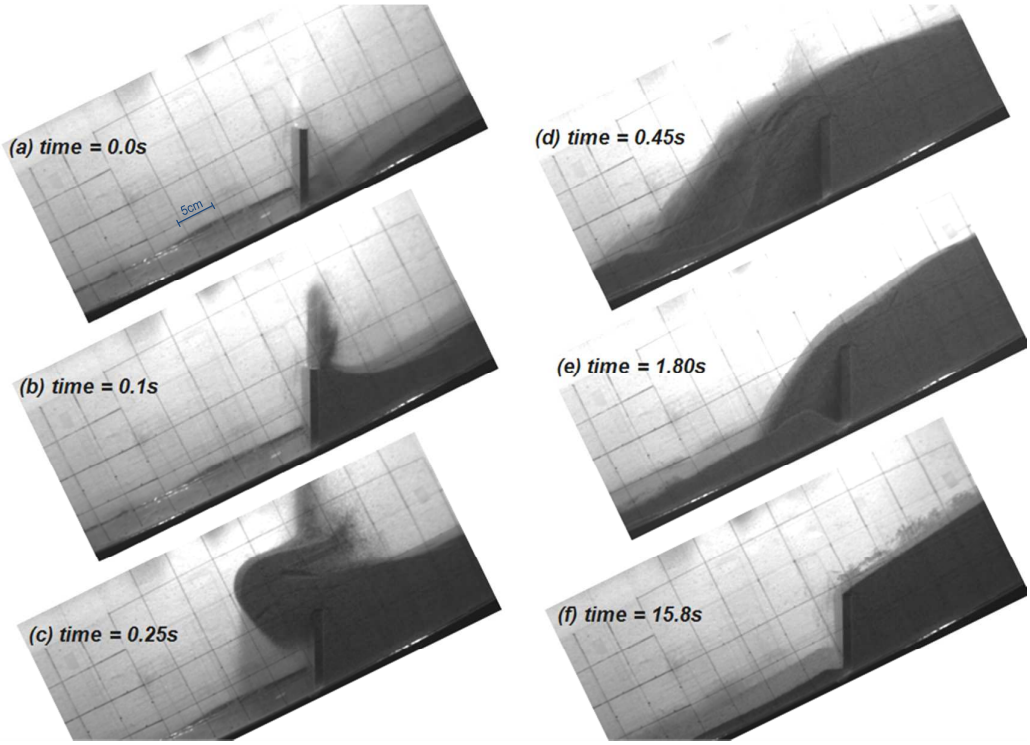

Fig. A1. High-speed camera images (Choi & Ng 2013)

Appendix B

Derivation of Equations (1) to (3)

Derivation of eq. (1) for calculation of x_i

Fig. B1 shows notations of different parameters relevant to debris overflow from barrier. x-coordinate of the trajectory path of landslide debris:

(B1) $x = v_m t$

where t is time after debris launches from the barrier crest and v_m is the maximum velocity of debris which cannot be trapped by barrier.

(B2) $y = h - ½ g t^2$

where g is gravitational acceleration.

Substitute eq. (B1) into (B2) to obtain the equation of the trajectory path of landslide debris:

(B3) $y = h - ½ g (x / v_m)^2$

Equation of the runout path:

(B4) $y = - tan\theta\, x$

Solve eq. (B3) and (B4) to obtain x_i,

(B5) $$x_i = \frac{v_m^2}{g}\left[\tan\theta + \sqrt{\tan^2\theta + \frac{2gh}{v_m^2}}\right]$$

Derivation of eqs. (2) and (3) for calculation of v_r and v_i

v_r can be estimated based on energy conservation principle, i.e.

(B6) $\frac{1}{2} m_r v_r^2 = KE_1 - KE_2 + m_r g (h + C_x x_i \tan \theta)$

where m_r = mass of debris overflow from barrier, v_r = velocity of remaining debris just before landing, KE_1 = total kinetic energy of debris before intercepted by barrier, and KE_2 = kinetic energy of debris retained by barrier.

The last term in eq. (B6) corresponds to potential energy gained in the ballistic flight. x_i is horizontal distance that landslide debris could travel, it is calculated using the maximum velocity of debris overflowing from barrier (see eq. (B1)). Since ratio of rear velocity to frontal velocity of overflowing debris varies, a correction factor C_x is proposed to establish an average value of x_i relevant to the energy calculation. The value of C_x depends on the ratio of the rear and frontal velocities of the overflowing debris, and can be calculated using eq. (B5) based on a combination of selected barrier height, debris velocity and inclination of runout profile with consideration of different velocity ratios. The leading portion of the debris flow typically has the highest velocity and kinetic energy. Therefore, the minimum spacing between barriers (x_i) should be calculated using the debris frontal velocity as presented in this study. However, the velocity of the rear portion of the overflow debris would be much slower. The use of the highest debris velocity as the initial condition of the debris mobility analysis of the next stage would result in grossly overestimation of the impact on the barrier downstream. It is suggested not design the overflow kinetic energy too conservative to avoid over-sizing of the barriers. Therefore, the attenuation of overflow debris mobility is considered. Fig. B2 shows a plot of C_x against velocity ratio. The data are generated based on combinations of a range of debris velocity up to 15 m/s, barrier heights of 1 m to 5 m, and ruout path inclinations of 20° to 60°. Values of C_x which envelop the upper limit of the data are recommended for using in the stage analysis (see also Table 1).

Eq. (B6) can be simplified to the following form:

(B7) $$v_{\mathrm{r}} = \sqrt{\frac{2\left[KE_r + m_r g\left(h + C_x x_i \tan\theta\right)\right]}{m_r}}$$

where $KE_r = KE_1 - KE_2$ (i.e. the kinetic energy of the overflow debris which can be obtain from debris mobility analysis).

v_r is velocity of remaining debris just before landing, it is in a direction tangential to the trajectory path. The velocity for inputting to the dynamic analysis of landslide debris at next stage (i.e. debris velocity after landing, v_i) is parallel to the inclination of the runout profile which can be calculated as follows:

Noting that β denotes angle between v_r and debris runout path (see Fig. B3), and $\beta + \theta$ is inclination of v_r to horizontal i.e.

(B8) $$\beta + \theta = \tan^{-1}\sqrt{\frac{m_r g\left(h + C_x x_i \tan\theta\right)}{KE_r}}$$ and

(B9) $$v_i = v_r \cos\beta$$

Combining eqs. (B8) and (B9) and applying velocity reduction factor (R) to account for the velocity reduction at landing, eq. (B10) is obtained:

(B10) $$v_{\mathrm{i}} = R v_r \cos\left[\left[\tan^{-1}\sqrt{\frac{m_r g\left(h + C_x x_i \tan\theta\right)}{KE_r}}\right] - \theta\right]$$

Figures

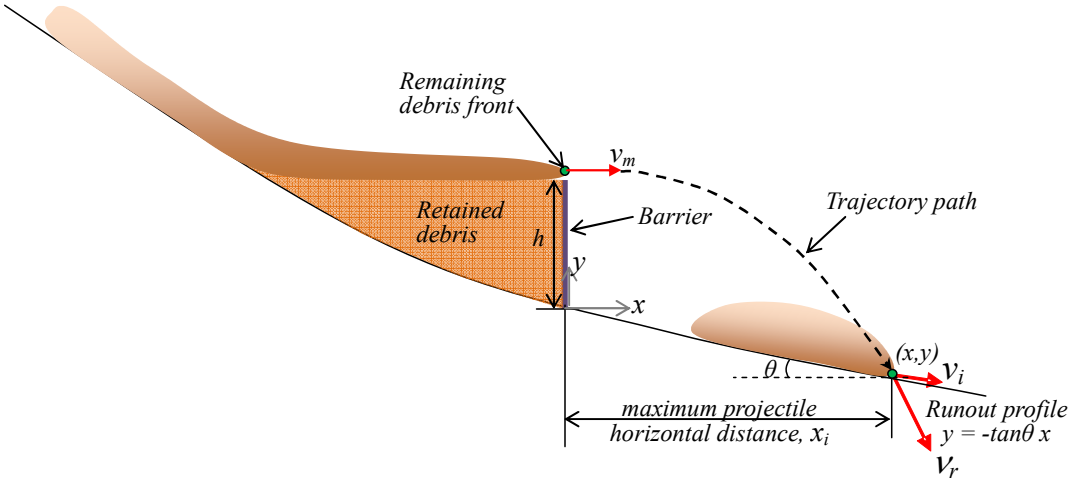

Fig. B1 Notations of different parameters relevant to debris overflows from barrier

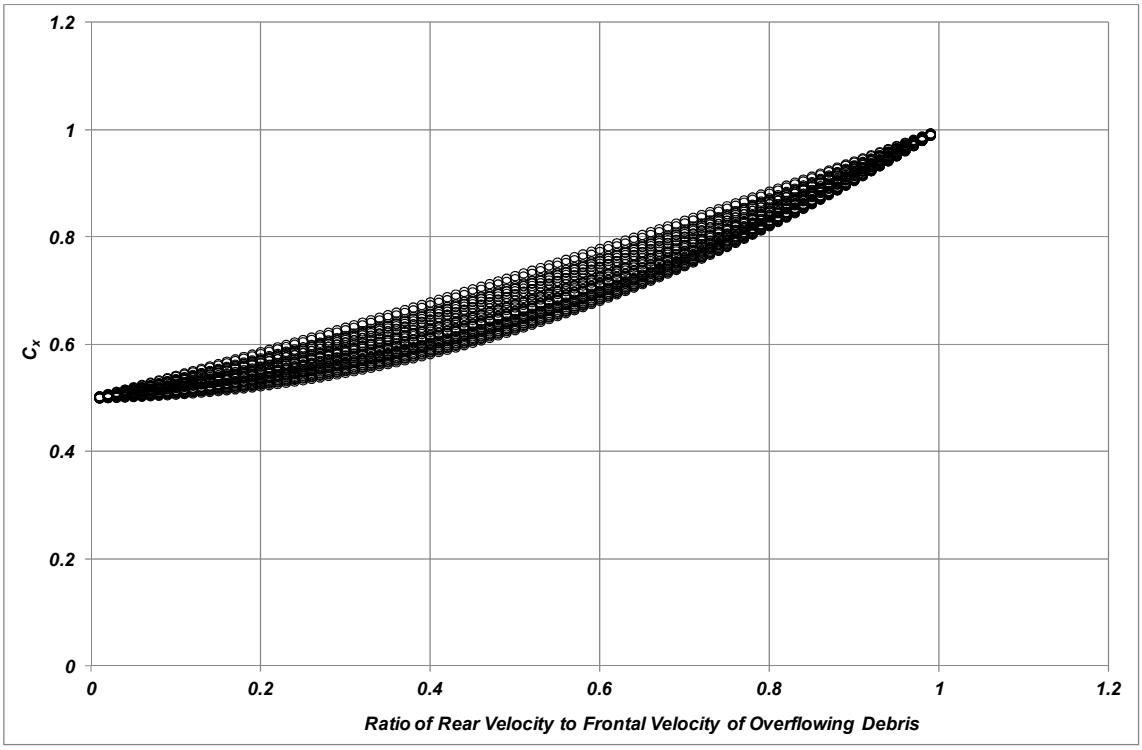

Fig. B2. Study of the value of C_x